



**HAL**  
open science

## Acute myeloid leukemia impairs natural killer cells through the formation of a deficient cytotoxic immunological synapse

Zena Khaznadar, Guylaine Henry, Niclas Setterblad, Sophie Agaugue, Emmanuel Raffoux, Nicolas Boissel, Hervé Dombret, Antoine Toubert, Nicolas Dulphy

### ► To cite this version:

Zena Khaznadar, Guylaine Henry, Niclas Setterblad, Sophie Agaugue, Emmanuel Raffoux, et al.. Acute myeloid leukemia impairs natural killer cells through the formation of a deficient cytotoxic immunological synapse. *European Journal of Immunology*, 2014, 43 (5), pp.1383-1388. 10.1002/eji.201444500 . hal-03664884

**HAL Id: hal-03664884**

**<https://u-paris.hal.science/hal-03664884>**

Submitted on 2 Jan 2023

**HAL** is a multi-disciplinary open access archive for the deposit and dissemination of scientific research documents, whether they are published or not. The documents may come from teaching and research institutions in France or abroad, or from public or private research centers.

L'archive ouverte pluridisciplinaire **HAL**, est destinée au dépôt et à la diffusion de documents scientifiques de niveau recherche, publiés ou non, émanant des établissements d'enseignement et de recherche français ou étrangers, des laboratoires publics ou privés.



Distributed under a Creative Commons Attribution 4.0 International License

## Acute myeloid leukemia impairs natural killer cells through the formation of a deficient cytotoxic immunological synapse

Zena Khaznadar,<sup>1,2</sup> Guylaine Henry,<sup>3</sup> Niclas Setterblad,<sup>4</sup> Sophie Agaugue,<sup>1</sup> Emmanuel Raffoux,<sup>5,6</sup> Nicolas Boissel,<sup>5,6</sup> Hervé Dombret,<sup>5,6</sup> Antoine Toubert,<sup>1-3</sup> and Nicolas Dulphy<sup>1-3</sup>

<sup>1</sup>Institut National de la Santé et de la Recherche Médicale (INSERM UMRS 1160), Paris, France

<sup>2</sup>Univ Paris Diderot, Sorbonne Paris Cité, Institut Universitaire d'Hématologie, Paris, France

<sup>3</sup>Assistance Publique–Hôpitaux de Paris (AP–HP), Hôpital Saint-Louis, Laboratoire d'Immunologie et Histocompatibilité, Paris, France

<sup>4</sup>Univ Paris Diderot, Sorbonne Paris Cité, Institut Universitaire d'Hématologie, Département d'Imagerie, Paris, France

<sup>5</sup>AP–HP, Hôpital Saint-Louis, Laboratoire d'Hématologie Adulte, Paris, France

<sup>6</sup>Univ Paris Diderot, Sorbonne Paris Cité, EA3518, Paris, France

**Key words:** NK cells; Immunological synapse; Acute myeloid leukemia; Cancer immunity

**Corresponding author:** Dr. Nicolas Dulphy, Hôpital Saint-Louis, 1, avenue Claude Vellefaux, 75475 Paris Cedex 10, France. Tel: +33-142494894. Fax: +33-142494641. nicolas.dulphy@univ-parisdiderot.fr

**Abbreviations:** AML acute myeloid leukemia. NCR natural cytotoxicity receptors.

NKIS NK immunological synapse. ROI region of interest. RRI relative recruitment index

Received: 24-Jan-2014; Revised: 30-Jun-2014; Accepted: 10-Jul-2014

This article has been accepted for publication and undergone full peer review but has not been through the copyediting, typesetting, pagination and proofreading process, which may lead to differences between this version and the Version of Record. Please cite this article as doi: 10.1002/eji.201444500.

This article is protected by copyright. All rights reserved.

**Abstract:**

Acute myeloid leukemia (AML) cells are killed by allogeneic NK cells. However, autologous NK cells from AML patients express decreased levels of activating receptors, and show reduced cytotoxicity. Here, we investigated how interactions between NK and AML cells might cause loss of NK cell activity in patients. Our results show that AML cell lines and primary blasts alter the NK cell phenotype, reducing their cytotoxic potential upon prolonged contact. Down-regulation of NK-cell-activating receptors was contact-dependent and correlated with conjugate formation. Time-lapse imaging of HL60 AML cell line and NK-cell interactions showed a high proportion of non-cytolytic contacts. Studies of NK-cell immunological synapses revealed a defect in lytic synapse formation. Namely, despite correct F-actin and LFA-1 recruitment, polarization of lytic granules toward primary blasts or AML cell lines was reduced. The NK-AML cell line synapses showed impairment of CD3 $\zeta$  recruitment. Attempts to correct these synapse defects by cytokine stimulation of NK cells improved conjugate formation, but not granule polarization. Pre-treatment of AML cell lines with the immuno-modulating molecule lenalidomide significantly enhanced granule polarization. We speculate that combining immunomodulatory drugs and cytokines could increase AML cell sensitivity to autologous NK cells and reinforce the activity of allogeneic NK cells in adoptive immunotherapy.

**Introduction:**

Natural killer (NK) cells are part of the innate immune system. They are regulated by a balance between signals from activating and inhibitory receptors [1]. NK cells mount highly effective anticancer immune responses, and thus represent major candidates for cancer immunotherapy [2]. Their ability to kill acute myeloid leukemia (AML) cells has been demonstrated by the absence of relapse after transplantation of allogeneic hematopoietic stem cells containing alloreactive NK cells [3]. Infusion of purified donor NK lymphocytes to consolidate engraftment after haplo-identical transplantation led to complete remission in some AML patients [4, 5]. Thus, NK cells are a potential tool for immunotherapy against AML [6, 7].

AML cells express ligands interacting with NK-cell activating receptors, making them susceptible to killing by NK cells [8, 9]. However, autologous NK cells do not effectively control AML growth in patients. Some mechanisms have been suggested for AML escape, including down-regulation of the ligands for NK-cell activating receptors, secretion of soluble forms of these ligands, or up-regulation of ligands for NK-cell inhibitory receptors [10]. Reduced toxicity has also been linked to down-regulation of activating receptors on NK cells, particularly NKG2D and the natural cytotoxicity receptors (NCR) NKp46 and NKp30 [11–13]. Upon remission, the NK-cell phenotype and function normalize, suggesting that the presence of AML blasts is responsible for the defects observed [12]. Interestingly, once out of the AML environment, NK cells that had previously expressed low levels of activating receptors regain their activity, becoming cytotoxic toward autologous leukemic blasts in mice [13]. This further implicates contact with AML cells in NK-cell activity down-modulation.

Interaction between NK cells and a cancerous cell involves a series of steps resulting in the formation of an immunological synapse (NKIS) [14]. Upon first contact, the NK-cell's cytoskeleton is reorganized in the zone of contact with the target cell [15]. Lytic granules are then polarized and their content released into the intercellular space, causing target cell death [16]. In this article, we hypothesized that AML-NK-cell interactions might alter the NK-cell phenotype, and reduce their cytotoxic potential upon prolonged contact. We therefore studied the results of interaction with AML cell lines or primary blasts on NK cells using in vitro functional assays complemented by imaging experiments focusing on the lytic NKIS.

**Results:****AML cells have a heterogeneous capacity to induce NK-cell degranulation**

NK-cell activation is mainly induced by interaction with ligands present on a target cell, such as leukemic blasts from AML patients. These blasts showed very variable ligand expression levels between patients (Fig. 1A), although all tested blasts expressed at least one ligand for NK-cell activating receptors. When allogeneic NK-cell degranulation was tested against leukemic cells from 24 AML patients, the level of degranulation induced was variable between patients, and did not correlate with the expression level of the ligands (Fig. 1B and data not shown). This suggested that the presence of activating receptors ligands is necessary but the relationship between their level of expression and capacity to activate NK-cell cytolytic function is not quantitative.

To reflect this variability in controlled experiments, we used two cell lines - THP1 and HL60 - expressing different NK-cell receptor ligands (Fig. 1A). Similar to the heterogeneity seen in NK-cell response to primary AML cells, NK cells from healthy donors degranulated more extensively when challenged with THP1 than with HL60 cells (Fig. 1B). No major differences were found to correlate with NK-cell activation for the ligands of NKG2D (MICA/B, ULBP1-3) or DNAM-1 (CD155 “PVR”), which were differentially expressed between the two cell lines. Although the expression patterns for these molecules was slightly different, the total ligand expression measured at the cell surface, using Fc recombinant proteins for each receptor, showed that this was not significant (Fig. 1A, 1C) [17]. Ligands of NKp30 and NKp46 were below the detection threshold with this method; while expression levels for HLA class I molecules, ligands for NK-cell inhibitory receptors, were identical on both cell lines (Fig. 1A). The THP1 and HL60 cells profiles were completed by measuring the expression levels of several AML phenotypic markers (CD33, CD34, CD45, CD117,

CD11b, CD11c) [18] and some suggested inhibitory molecules (CD137L, CD200, CD273, CD274, and CD276) [19–21]. This revealed no major differences (Supporting Information Fig. 1). Only expression of the co-stimulatory pair LFA-1/ICAM-1 (CD11a/CD54) differed between THP1 and HL60 cells, with THP1 cells expressing significantly higher levels of CD54 and HL60 cells expressing CD11a, as expected for an acute promyelocytic leukemia cell line (Fig. 1C) [22].

### Contact with AML cells alters NK-cell phenotype and function

With the hypothesis that AML cells could promote NK-cell deficiencies observed in patients [10–13], we proceeded to test whether these defects could be reproduced *in vitro* by co-culture of healthy donor NK cells with AML cell lines. First, we compared expression of activating receptors (NKG2D, DNAM-1 and NKp46) after cultivating PBMCs alone or with THP1 or HL60 cells for 48 h. DNAM-1 expression decreased with both cell lines, whereas NKG2D expression was reduced by 45% with THP1 cells only. Interestingly, for NKp46 we noted a trend with THP1 cells (*p*-value 0.05) but the decrease was not significant with HL60 cells (Fig. 2A). A greater fold-decrease was observed with higher AML/PBMC ratios (data not shown). Co-culture experiments performed as control with the non-myeloid, lymphoma cell line RAJI showed no effect on DNAM-1 or NKG2D expression on NK cells and a down-regulation of NKp46 (Fig. 2A).

We next assessed NK-cell degranulation capacity after co-culture with AML cell lines. To do this, CD107a-mobilization assays with a HLA class-I-negative target (K562) were performed (Fig. 2B). Exposure to HL60 cells very slightly reduced NK-cell degranulation, whereas contact with THP1 cells severely decreased degranulation (16.8% vs. 43.4% for PBMC cultured alone, *p*=0.03).

When performing degranulation tests with primary AML blasts (Fig. 1B) the NKG2D level on NK cells decreased, and the degree of degranulation correlated with the extent of this down-regulation (Fig. 2C). Interestingly, NKG2D expression was reduced on CD107a<sup>-</sup> NK cells, suggesting that down-regulation of this receptor requires contact, but not necessarily degranulation. Taken together, these experiments demonstrated that AML cells can dampen the expression of activating receptors while also reducing the cytolytic activity of fresh allogeneic NK cells. In line with differences in conjugate formation assays - where NK cells formed twice as conjugates with THP1 as with HL60 cells (Fig. 2D) - the two cell lines differed in their effects on NK cells overall. THP1 cells generally had a more severe impact than HL60 cells. These data thus suggest that NK-cell inhibition could be the result of the number of NK/AML cells interactions.

We therefore tested whether contact with primary AML blasts had the same adverse effect as cell lines on healthy NK cells. PBMCs from three unrelated healthy donors were cultivated with AML blasts isolated from four untreated patients. The NK-cell phenotype after 48 h showed a slight decrease in NKp46 in all cases. AML cells from patients showed the same variability in their effect on NK cells with some patients (Pt3 and Pt4) causing a significant reduction in DNAM-1 (34%) and NKG2D (16%) expression (Fig. 2E). When tested for conjugate formation, blasts from these same patients formed a higher percentage of conjugates with NK cells than blasts from the other two patients (Fig. 2E). After co-culture with patient blasts, higher expression of both DNAM1 and NKG2D on NK cells correlated negatively with the number of conjugates formed by those cells (Fig. 2F). Expression levels of NKG2D and DNAM-1 ligands on blasts from the 4 patients did not relate to the receptors down-regulation. And phenotyping for the inhibitory molecules did not show a difference between the different AML cells (Supporting Information Table 1).

Soluble factors secreted by AML cells have been shown to inhibit NK-cell proliferation and are thought to be responsible for NK-cell receptor down-regulation in patients [12, 23, 24]. However, in our hands, exposing PBMCs to cell lines or primary blasts supernatants had no effect on NK-cell phenotype (data not shown).

### **Low killing rate upon NK cell-AML cell line interaction**

Since contact was needed to induce changes in NK cells, we investigated whether AML cell lines could affect the dynamics and outcome of NK-cell interaction [25].

Target cells (K562 or HL60) were seeded into a multi-chamber culture dish in medium supplemented with a nucleic-acid stain. Due to their high motility, THP1 cells were not suitable for analysis in these experiments as they would be difficult to track on successive images. NK cells were pre-activated with IL-15, labeled and added to the chamber (NK/AML ratio 2:1), and interactions with target cells were scored. HL60 cells were engaged in a lower number of interactions with NK cells than K562 cells, with 72% of tracked HL60 cells taking part in interactions with NK cells versus 93% of K562 cells (Fig. 3A). This was consistent with the flow cytometry results for conjugate formation (Fig. 3B).

To assess the efficacy of NK-cell killing, we measured the Conjugate-Kill time, i.e., the time between conjugate formation and fluorescence appearing in target cells as explained in the *Materials and methods* section (Fig. 3C, and Supporting Information Video 1). NK cells required an average of 5 min 6 sec to kill K562 cells, and 4 min 54 sec to kill HL60 cells (Fig. 3D). The difference was not significant. Some target cells were more resistant, requiring multiple lytic hits before dying. Analysis of the population dying only after contact with two NK cells (Supporting Information Fig. 2A) also showed no difference in time to death based

on the identity of the target: average times were 12 min for K562 and 11 min 42 sec for HL60 for the first contact, and 2 min 54 sec and 3 min 42 sec, respectively, for the second contact (Fig. 3E, and Supporting Information Video 2). Thus, the time needed for NK cells to kill target cells was no different for AML cells than for the “gold standard” of killing efficiency, K562 cells. Ineffective interactions were defined as contacts that detached after more than 5 min or lasted up to 30 min without inducing apoptotic changes in the target cell (Supporting Information Fig. 2B, and Supporting Information Video3). NK interactions with HL60 were considerably less effective, with 26% of HL60 cells resisting lysis, than interactions with K562 cells, where only 15% of cells were not killed after interaction (Fig. 3F, 3G). Thus, the overall outcome of NK cells-AML cell lines interaction was reduced cell death, with a smaller number of HL60 cells lysed after contact with NK cells.

#### **NK-AML immunological synapse shows defective lytic granule polarization**

The low killing rate for NK-AML interactions described above suggests that AML cells engage NK cells in lytic interactions which are never completed. To investigate how this occurs, we analyzed the lytic NKIS formed in this context [26].

Depending on how the balance between activating and inhibitory signals tips, NK cells form two types of NKIS: inhibitory synapses, where actin reorganization is blocked, lytic granules are not polarized to the synapse, and the targeted cell is not killed [27]; and lytic synapses, where the NK-cell actin cytoskeleton reorganizes at the synapse and lytic granules become polarized for the directed secretion of their contents onto the target cell [14]. Indeed the use of MHCI transfected K562 cells reduced NK-cell degranulation in a CD107a test constantly with K562-E cell line and to a lesser point with K562-Cw\*03:04 (Supporting Information Fig. 3). However when we examined synapses showing actin reorganization in the contact area i.e., lytic synapses, lytic granule polarization was not significantly different from MHCI-

negative K562 cells (Fig. 4A, 4B), thus ruling out a straightforward inhibition due to MHC I interaction with inhibitory receptors. NKIS formed with AML cell lines were then compared with those formed with K562 cells. With AML cell lines, a reduced percentage of NK-cell conjugates contained polarized CD107a<sup>+</sup> lytic granules (Fig. 4A, 4B). A similar effect on polarization was found with primary leukemic cells bound to healthy donor NK cells (Fig. 4B, 4C).

In lytic synapses, recruitment of LFA-1 integrin to the synapse provides an activation signal, and is necessary for lytic granule polarization [28, 29]. Inhibitory signals disrupt NK cell adhesion and granule polarization via LFA-1 [30, 31]. To test CD11a (LFA-1 $\alpha$  subunit) recruitment to the NK immunological synapse, a relative recruitment index (RRI) was calculated for conjugates. This showed that CD11a was correctly recruited to NK-AML cells synapses (Fig. 5A,B). Due to the higher expression of CD11a on HL60 cells (Fig. 1), NK-HL60 cells interactions had a higher RRI than NK-THP1 cells and NK-K562 cells interactions.

Since signaling through NCRs is partially responsible for granule polarization [32], we next examined CD3 $\zeta$  polarization as an indicator of NCR (NKp46, NKp30) recruitment to the synapse area [33, 34]. NK-AML cell lines synapses are associated with little or no recruitment of CD3 $\zeta$  compared with NK-K562 synapses (Fig. 5C, 5D). Co-staining for CD107a and CD3 $\zeta$  showed that when CD3 $\zeta$  was recruited lytic granule polarized to the NK-AML synapse, whereas with NKIS lacking CD3 $\zeta$  recruitment (RRI<2) almost no lytic granule polarization was observed (Fig. 6). This reveals a direct relationship between defective NK-cell activation via CD3 $\zeta$ -associated receptors and the uncompleted NKIS.

## **Immuno-modulating drugs, but not cytokines, increase lytic granule polarization in the NKIS**

If allogeneic NK cells are to be used in adoptive immunotherapy strategies, the resistance of AML cells to NK-mediated lysis must be overcome [6, 7]. We therefore tested whether pre-activating NK cells with IL-2 or IL-15 overnight improved lytic granule polarization in this context. Pre-activation significantly increased the number of NK cells interacting with AML cell lines, with a higher percentage of conjugates formed with both THP1 and HL60 cells, and as a result increased degranulation (Fig. 7A, 7B). However, the NKIS remained defective as lytic granule polarization was not significantly restored (Fig. 7C).

We next tried treating AML cell lines with the immuno-modulating drug lenalidomide. Lenalidomide is an interesting candidate because it has been effective in some AML cases [35, 36]. A proposed mechanism of this molecule is increasing the expression of NK-activating receptor ligands on cancer cells [37–39]. In a very similar context, lenalidomide was able to correct defects in the formation of T-cell lytic synapses with leukemic cells [20]. With NK cells, with a concentration corresponding to the dose used in trials for treating refractory AML [35, 36], lenalidomide treatment significantly increased polarization of lytic granules in NKIS, both with THP1 and HL60 cells (Fig. 7D). However NKG2D and DNAM-1 ligands levels of expression did not change with lenalidomide treatment nor did the level of any of the studied inhibitory molecules: CD137L, CD200, CD273, CD274, and CD276 (Supporting Information Fig. 4).

**Discussion:**

AML cells express ligands for NK cell-activating receptors [8, 9, 40]. This makes them potential targets for NK-lysis [13]. However, NK cells do not kill autologous leukemic blasts or prevent leukemia development. In most patients this is due to low-level surface expression of NK-activating receptors [10–13]. Normalization of NK cells upon remission and the return of NK cells' ability to kill autologous AML cells in mice suggest that the defect is not due to a problem with NK cells themselves, but rather results from contact with AML cells [12, 13]. Interestingly, AML cells from patients with low NCR expression are highly susceptible to lysis by NK cells expressing normal levels of NCRs [11], thus indicating that AML cells are not simply resistant to NK-cell cytotoxicity. Combining these observations, it appears that a point may occur during AML development when normal cytotoxic NK cells become overwhelmed by the number of target AML cells, and start losing their functionality.

In this study, through observations from an integrated system of NK-cell functions and imaging, we propose a model of escape where, instead of avoiding contact, AML cells actively engage NK cells in ineffective interactions. In support of this, NK cells from healthy donors partially lost activity after interactions with AML cells (Supporting Information Video 4) [41–43]. In addition, a significant percentage of NK- HL60, an AML cell line, interactions did not result in lysis, thus interaction can decrease NK cell activity without killing the target cell. Our results indicate that inefficient killing was the result of qualitative impairment of the immunological synapse.

Direct cell-cell contact is necessary to produce NK-cell defects, with conjugate formation causing down-regulation of receptors activating NK cells, such as NKG2D, DNAM-1 and NKp46, and subsequently impairing cytotoxicity. Among the cell lines tested, THP1

expresses higher levels of the adhesion molecule CD54 (ICAM-1), which binds to LFA-1. This pairing mediates NK-cell conjugate formation [44]. In our assays, THP1 effectively formed more conjugates with NK cells, leading to more severe perturbations. However, on patient cells, although considerable variations in CD54 expression levels were noted, this did not correlate with an impaired NK-cell degranulation capacity upon contact (data not shown).

Cytotoxicity is the final outcome of NK-target cell interactions, but dynamic results showed a low killing rate for NK-HL60 cell conjugates, this stemmed from a high rate of uncompleted interactions between NK cells and AML cells. When the interaction did proceed to completion, the time required by NK cells to recruit lytic granules, release their contents and lyse the leukemic cell was unchanged compared with other target cells. A similar result was recently reported for target lysis via antibody-dependent cellular cytotoxicity [45].

To kill, NK cells must direct their lytic granules toward the target cell, where their contents can be released to induce its effect [14]. NKIS with AML cells showed a normal accumulation of F-actin, the hallmark of lytic synapses, but a low rate of lytic granule polarization. Similar immature cytotoxic synapses have been described with anti-tumor T cells [46, 47]. It was previously known that polarization and exocytotic signals can be uncoupled in NK cells [29]; our findings show that cytoskeleton polarization and lytic granule polarization can also be uncoupled. Different signaling proteins are involved in these two steps of NKIS formation. Inhibition of a MAP kinase, JNK-1, or of (WASp)-interacting protein (WIP) has been shown to inhibit polarization of lytic granules to the immune synapse, but had no effect on conjugate formation or localization of actin at the synapse [48, 49]. Most studies on NKIS have been conducted using coated surfaces or cell lines expressing ligands for only one or two NK-activating or inhibitory receptors, and mostly with NK leukemic-like cell lines, such as NK92 or NKL, as effectors. Using AML cell lines expressing a wide range of activating and

inhibitory ligands and primary polyclonal NK cells better reflects the disease conditions. Thereby the dissociation seen in our experiments suggests that each step in NKIS formation requires a particular level of activation, determined by the number and type of inhibitory and stimulatory ligands engaged with their receptors.

The activation signal necessary for lytic granule polarization is provided by recruitment of the integrin LFA-1 to the synapse [28, 50]. KIR-mediated inhibitory signals can disrupt NK-cell adhesion and granule polarization via LFA-1 [30, 31]. However, these appear not to be responsible for the defective NK-AML synapse described here, as LFA-1 is correctly recruited. Staining for inhibitory molecules reported to impair T-cell cytotoxic synapse formation (CD200, CD273, CD274, and CD276) [19, 20], revealed the presence of CD200 on the AML cell lines and the primary blasts studied (Supporting Information Fig. 1 and Supporting Information Table 1). In AML, CD200 expression is associated with poor outcome, with CD200<sup>high</sup> patients showing reduced NK-cell activity and NCR expression [19].

Lytic granule polarization is triggered by CD3 $\zeta$  recruitment, this signaling adaptor combines with NKp46 to transmit its signal to the MAP kinase JNK1 [32]. NK-AML cell lines synapses generally recruited very little or no CD3 $\zeta$ , another indication of their non-activated state. In NK-AML synapses where CD3 $\zeta$  was not recruited, NK cells exhibited no polarization of lytic granules, revealing a direct relationship between defective NK-cell activation and uncompleted NKIS, highlighting the importance of CD3 $\zeta$  in killing AML cells. Chronic NKG2D stimulation due to disease-related ligand expression has been shown to trigger CD3 $\zeta$  degradation [51]. This could contribute to impairing NK-cell activity upon long term interactions. Thereby NKIS defects can be the result of higher inhibition with molecules like CD200 and/or lower activation through CD3 $\zeta$ .

Some NK-cell defects could be overcome by pre-activation with cytokines (IL-2, IL-15), which increased conjugate formation and degranulation, but did not improve synapse formation. More promisingly, pre-treatment of AML cell lines with the immuno-modulating molecule lenalidomide improved the polarization rate significantly. A possible mechanism is a decrease in The TNF family member receptor activator for NF- $\kappa$ B ligand (RANKL).

Lenalidomide has been shown to decrease RANKL in bone marrow [52]. RANK signaling into NK cells directly impairs NK-cell anti-leukemia reactivity [53]. Combining the correcting effect of lenalidomide on NKIS with the qualitative effect of cytokines on conjugate formation could increase AML cell sensitivity to autologous NK and reinforce the activity of allogeneic NK cells in adoptive immunotherapy.

## **Materials and methods:**

### **Cell isolation and cell lines**

PBMCs were isolated from healthy donor samples obtained from the French blood service (EFS). NK cells were isolated by negative selection using a NK-cell Isolation Kit (Miltenyi Biotec). Purified NK cells were used without any prior culture or exposure to growth factors for all experiments except when preactivation with IL-2 or IL-15 is mentioned.

All cell lines (THP1: human acute monocytic leukemia; HL60: human acute promyelocytic leukemia cell line; controls: K562, K562-Cw\*0304 transfected to express HLA-C, and K562-E2B4 transfected to express HLA-E [54]) were grown in RPMI supplemented with 10% FBS, and L-glutamine, sodium pyruvate, hepes buffer (1% each), and with the corresponding selection agent for transfected cells. The expression of HLA molecules on transfected cell lines was verified by flow cytometry.

All patients gave written informed consent to participate in this study, the protocol for which was approved by the local review board in line with the Declaration of Helsinki. Samples from patients with AML were collected at diagnosis in the Hematology Department of Saint-Louis Hospital, Paris, France, before treatment. CD33<sup>+</sup> blasts were isolated by positive sorting from PBMCs using the StemSep System (StemCell-Technology).

### **Flow cytometry**

Ligands for NKG2D, DNAM-1, NKp30 and NKp46 were stained with Fc recombinant proteins for each receptor (R&D system) and revealed using a Biotin-conjugated F(ab')<sub>2</sub> goat anti-human IgG (Jackson ImmunoResearch) followed by streptavidin R PE (Molecular probes). Monoclonal antibodies (mAbs) used to stain AML and NK cells were: ULBP1, ULBP2, ULBP3, MICA, MICB, CD155 “PVR” from R&D system; CD112 “Nectin2”,

CD276 “B7H3”, CD137L, CD117, CD200, CD11c, HLA-E, DNAM-1 from Biolegend; CD11a, CD273 “PDL-2”, CD34, CD11b, CD54, HLA-A,B,C, CD3, CD33, CD56, CD16, IFN- $\gamma$ , an isotype control from BD biosciences; CD45 (Invitrogen); CD33, NKp46, NKG2D from Beckman Coulter; and CD274 “PD-L1”(ebioscience).

Flow cytometry analysis was performed on a FACSDiva (BD), and results were analyzed using Diva v6.1.3 or FlowJo vX.0.6 software.

### **Conjugation and NK-cell degranulation assays by flow cytometry**

Conjugation tests were performed with purified NK cells stained with CellTracker Green (CMFDA) and AML cells stained with CellTracker Orange (CMRA) (Molecular Probes) according to the manufacturer's instructions. Cells were mixed 1:1 and incubated for 1 h at 37 °C. Percentage of bicolor cell-conjugates among CMFDA positive cells was measured.

NK cells were incubated overnight with target cells. Degranulation was then estimated by measuring the percentage of CD107a-positive cells [55].

### **Time-lapse microscopy**

Microscopy was performed in culture conditions at 37 °C under 5% CO<sub>2</sub> on a on a NIKON Biostation timelapse microscope equipped with a 40 $\times$  N.A 0.8 using the Biostation IM software (Nikon). Target cells, 1.5 $\times 10^5$  K562 or HL60 cells, were seeded onto two different segments of a Hi-Q4 Culture Dish (Ibidi), previously coated with 1% collagen (Sigma Aldrich)/2% fibronectin (Gibco), and left to adhere for at least 2 hours. Sytox Blue Nucleic-Acid Stain (Molecular Probes) was added to the medium at 5  $\mu$ M. After choosing two fields of interest per segment at 40 $\times$  magnification, 3 $\times 10^5$  CMRA-labeled NK cells were added to each segment (NK:Target ratio 2:1) and imaging was started simultaneously for the two target cells. Images were acquired on three channels (Phase-contrast, DAPI and TRITC filter cubes) every 45 sec for 3 hours. Images were analyzed using BioStation software and the Fiji

package [56]. Target cells were manually tracked, and each interaction with an NK cell was scored. Conjugates were defined as physical contact between NK cells and target cells lasting longer than 2 min 15 sec (3 imaging cycles). Target cell death was detected by the gradual appearance of Sytox Blue fluorescence, and by visual signs of death in the phase-contrast image (blebbing).

### **Fluorescence microscopy and image analysis**

Slides of cell conjugates (NK:AML ratio 2:1) were mounted as follows: purified NK cells and AML cells were incubated together for 1 hour at 37 °C, resuspended gently, seeded on slides previously coated with poly-L-lysine (Sigma Aldrich) and left to adhere for 30 min at 37 °C. Cells were fixed in 4% paraformaldehyde at room temperature, permeabilized with 0.1% saponin, and non-specific sites were blocked with TBS-T 5% BSA. Cells were labeled for 30 min to reveal CD107a (H4A3-FITC, BD or H4A3-Brilliant Violet421, Biolegend), LFA1 (HI111-FITC, BD Pharmingen), and F-actin (Phalloidin Alexa Fluor568, Molecular Probes), or for 1 hour to reveal CD3 $\zeta$  (6B10.2-FITC, Biolegend) and with the isotype control. Slides were washed with TBS-T 1% BSA, mounted with hard-set Vectashield with or without DAPI (Vector Laboratories).

Polarization of lytic granules was scored under an Axiovert 200M microscope (Zeiss) for at least 50 conjugates per slide in randomly selected fields. Conjugates were defined based on morphology - when opposing NK cell and target cell membranes appeared flat, with accumulated F-actin. Conjugates were considered polarized when CD107a-positive lytic granules were located in the NK cell quarter nearest the target cell [32, 48]. Results were validated by a second examiner who re-counted randomly selected slides. Representative images were captured with Axiovert 200M microscope equipped with a Plan Apochromat 63X/N.A.1.4 oil-immersion objective, an optavar 1.6 $\times$  lens (resulting magnification 100.8 $\times$ )

and an Axiocam MRM camera (Zeiss) using the Axiovision v4.5.0.0 software (Zeiss), or with LSM 510 confocal microscope (Zeiss) equipped with a 64× oil-immersion objective and optavar 4× lens using the associated software.

The Fiji package was used to analyze fluorescence microscopy images [56]. On unprocessed images for actin, LFA1 and CD3ζ, a region of interest (ROI).1 was defined on the NK cell membrane touching the target cell. ROI.2 was located on the opposing NK-cell membrane, and ROI.3 was in the background. The mean gray value (MGV) was measured for each ROI. A relative recruitment index (RRI) was calculated based on:  $RRI = (MGV_{ROI.1} - MGV_{ROI.3}) / (MGV_{ROI.2} - MGV_{ROI.3})$

### **Cytokines and lenalidomide treatment**

Where indicated, purified NK cells were incubated overnight in medium supplemented with rhIL-2 1000 IU/mL or rhIL-15 10 ng/mL (ImmunoTools), prior to performing degranulation, conjugate and polarization tests as described. In other assays, lenalidomide (LC Laboratories) was added to AML cell cultures at a final concentration of 10 μM 18-24 hours before assessing lytic granule polarization as described. Granule polarization was counted on blinded slides.

### **Statistics**

Statistics and graphical presentations were produced using GraphPad Prism5 software (GraphPad). Wilcoxon's signed rank test was used to compare NK cells in microscopy experiments or after co-culture and to compare results after cells treatments (cytokines/lenalidomide). Other data were compared using the Mann-Whitney test.

**Acknowledgements:**

This work was supported by research grants from the Association Laurette Fugain, Association pour la Recherche sur le Cancer (Z.K, #DOC20100600956), Fondation pour la Recherche Médicale (S.A, #SPF20100518400), Fondation de France (S.A, #2012-26957), Institut National du Cancer (grants #R8S09081HHA, #RPT12008HHA), and Assistance Publique–Hopitaux de Paris (A.T, Translational Research grant in Biology 2010, #RTB10002).

**Conflict of interest**

The authors declare no commercial or financial conflict of interest.

**References:**

1. **Caligiuri MA.** Human natural killer cells. *Blood.* 2008. **112**:461–469.
2. **Ljunggren H-G, Malmberg K-J.** Prospects for the use of NK cells in immunotherapy of human cancer. *Nat Rev Immunol.* 2007. **7**:329–339.
3. **Ruggeri L, Mancusi A, Burchielli E, Perruccio K, Aversa F, Martelli MF, Velardi A.** Natural killer cell recognition of missing self and haploidentical hematopoietic transplantation. *Semin. Cancer Biol.* 2006. **16**:404–411.
4. **Miller JS, Soignier Y, Panoskaltsis-Mortari A, McNearney SA, Yun GH, Fautsch SK, McKenna D, et al.** Successful adoptive transfer and in vivo expansion of human haploidentical NK cells in patients with cancer. *Blood.* 2005. **105**:3051–3057.
5. **Passweg JR, Tichelli A, Meyer-Monard S, Heim D, Stern M, Kühne T, Favre G, et al.** Purified donor NK-lymphocyte infusion to consolidate engraftment after haploidentical stem cell transplantation. *Leukemia.* 2004. **18**:1835–1838.
6. **Farag SS, Caligiuri MA.** Immunologic Approaches to Acute Leukemia in the Elderly. *Seminars in Hematology.* 2006. **43**:118–125.
7. **Vey N, Bourhis J-H, Boissel N, Bordessoule D, Prebet T, Charbonnier A, Etienne A, et al.** A phase 1 trial of the anti-inhibitory KIR mAb IPH2101 for AML in complete remission. *Blood.* 2012. **120**:4317–4323.
8. **Salih HR, Antropius H, Gieseke F, Lutz SZ, Kanz L, Rammensee H-G, Steinle A.** Functional expression and release of ligands for the activating immunoreceptor NKG2D in leukemia. *Blood.* 2003. **102**:1389–1396.
9. **Pende D, Spaggiari GM, Marcenaro S, Martini S, Rivera P, Capobianco A, Falco M, et al.** Analysis of the receptor-ligand interactions in the natural killer-mediated lysis of freshly isolated myeloid or lymphoblastic leukemias: evidence for the involvement of the Poliovirus receptor (CD155) and Nectin-2 (CD112). *Blood.* 2005. **105**:2066–2073.
10. **Lion E, Willemen Y, Berneman ZN, Van Tendeloo VFI, Smits ELJ.** Natural killer cell immune escape in acute myeloid leukemia. *Leukemia.* 2012. **26**:2019–2026.
11. **Costello RT, Sivori S, Marcenaro E, Lafage-Pochitaloff M, Mozziconacci M-J, Reviron D, Gastaut J-A, et al.** Defective expression and function of natural killer cell-triggering receptors in patients with acute myeloid leukemia. *Blood.* 2002; **99**:3661–3667.
12. **Fauriat C, Just-Landi S, Mallet F, Arnoulet C, Sainty D, Olive D, Costello RT.** Deficient expression of NCR in NK cells from acute myeloid leukemia: Evolution during leukemia treatment and impact of leukemia cells in NCRdull phenotype induction. *Blood.* 2007. **109**:323–330.

13. **Siegler U, Kalberer CP, Nowbakht P, Sendelov S, Meyer-Monard S, Wodnar-Filipowicz A.** Activated natural killer cells from patients with acute myeloid leukemia are cytotoxic against autologous leukemic blasts in NOD/SCID mice. *Leukemia*. 2005. **19**:2215–2222.
14. **Orange JS.** Formation and function of the lytic NK-cell immunological synapse. *Nat. Rev. Immunol.* 2008. **8**:713–725.
15. **Wulfig C, Purtic B, Klem J, Schatzle JD.** Stepwise cytoskeletal polarization as a series of checkpoints in innate but not adaptive cytolytic killing. *PNAS*. 2003. **100**:7767–7772.
16. **Mace EM, Wu WW, Ho T, Mann SS, Hsu H-T, Orange JS.** NK Cell Lytic Granules Are Highly Motile at the Immunological Synapse and Require F-Actin for Post-Degranulation Persistence. *J. Immunol.* 2012. **189**:4870–4880.
17. **Mamessier E, Sylvain A, Bertucci F, Castellano R, Finetti P, Houvenaeghel G, Charaffe-Jaufret E, et al.** Human Breast Tumor Cells Induce Self-Tolerance Mechanisms to Avoid NKG2D-Mediated and DNAM-Mediated NK Cell Recognition. *Cancer Research*. 2011. **71**:6621–6632.
18. **Miguel JFS, Vidriales MB, López-Berges C, Díaz-Mediavilla J, Gutiérrez N, Cañizo C, Ramos F, et al.** Early immunophenotypical evaluation of minimal residual disease in acute myeloid leukemia identifies different patient risk groups and may contribute to postinduction treatment stratification. *Blood*. 2001. **98**:1746–1751.
19. **Coles SJ, Wang ECY, Man S, Hills RK, Burnett AK, Tonks A, Darley RL.** CD200 expression suppresses natural killer cell function and directly inhibits patient anti-tumor response in acute myeloid leukemia. *Leukemia*. 2011. **25**:792–799.
20. **Ramsay AG, Clear AJ, Fatah R, Gribben JG.** Multiple Inhibitory Ligands Induce Impaired T Cell Immunological Synapse Function in Chronic Lymphocytic Leukemia That Can Be Blocked with Lenalidomide. *Blood*. 2012. **120**:1412–1421.
21. **Baessler T, Charton JE, Schmiedel BJ, Grünebach F, Krusch M, Wacker A, Rammensee H-G, et al.** CD137 ligand mediates opposite effects in human and mouse NK cells and impairs NK-cell reactivity against human acute myeloid leukemia cells. *Blood*. 2010. **115**:3058–3069.
22. **Zhou Y, Jorgensen JL, Wang SA, Ravandi F, Cortes J, Kantarjian HM, Medeiros LJ, et al.** Usefulness of CD11a and CD18 in Flow Cytometric Immunophenotypic Analysis for Diagnosis of Acute Promyelocytic Leukemia. *AJCP*. 2012. **138**:744–750.
23. **Bergmann L, Schui DK, Brieger J, Weidmann E, Mitrou PS, Hoelzer D.** The inhibition of lymphokine-activated killer cells in acute myeloblastic leukemia is mediated by transforming growth factor-beta 1. *Exp. Hematol.* 1995. **23**:1574–1580.
24. **Orleans-Lindsay JK, Barber LD, Prentice HG, Lowdell MW.** Acute myeloid leukaemia cells secrete a soluble factor that inhibits T and NK cell proliferation but not

cytolytic function--implications for the adoptive immunotherapy of leukaemia. *Clin. Exp. Immunol.* 2001. **126**:403–411.

25. **Vanherberghen B, Olofsson PE, Forslund E, Sternberg-Simon M, Khorshidi MA, Pacouret S, Guldevall K, et al.** Classification of human natural killer cells based on migration behavior and cytotoxic response. *Blood.* 2013. **121**:1326–1334.

26. **Orange JS, Harris KE, Andzelm MM, Valter MM, Geha RS, Strominger JL.** The mature activating natural killer cell immunologic synapse is formed in distinct stages. *PNAS.* 2003. **100**:14151–14156.

27. **Eissmann P, Davis DM.** Inhibitory and regulatory immune synapses. *Curr. Top. Microbiol. Immunol.* 2010. **340**:63–79.

28. **Barber DF, Faure M, Long EO.** LFA-1 Contributes an Early Signal for NK Cell Cytotoxicity. *J Immunol.* 2004. **173**:3653–3659.

29. **Bryceson YT, March ME, Barber DF, Ljunggren H-G, Long EO.** Cytolytic granule polarization and degranulation controlled by different receptors in resting NK cells. *J. Exp. Med.* 2005. **202**:1001–1012.

30. **Burshtyn DN, Shin J, Stebbins C, Long EO.** Adhesion to target cells is disrupted by the killer cell inhibitory receptor. *Current Biology.* 2000. **10**:777–780.

31. **Das A, Long EO.** Lytic Granule Polarization, Rather than Degranulation, Is the Preferred Target of Inhibitory Receptors in NK Cells. *The Journal of Immunology.* 2010. **185**:4698 – 4704.

32. **Chen X, Trivedi PP, Ge B, Krzewski K, Strominger JL.** Many NK cell receptors activate ERK2 and JNK1 to trigger microtubule organizing center and granule polarization and cytotoxicity. *PNAS.* 2007. **104**:6329 –6334.

33. **Pessino A, Sivori S, Bottino C, Malaspina A, Morelli L, Moretta L, Biassoni R, et al.** Molecular cloning of NKp46: a novel member of the immunoglobulin superfamily involved in triggering of natural cytotoxicity. *J. Exp. Med.* 1998. **188**:953–960.

34. **Pende D, Parolini S, Pessino A, Sivori S, Augugliaro R, Morelli L, Marcenaro E, et al.** Identification and molecular characterization of NKp30, a novel triggering receptor involved in natural cytotoxicity mediated by human natural killer cells. *J. Exp. Med.* 1999. **190**:1505–1516.

35. **Fehniger TA, Byrd JC, Marcucci G, Abboud CN, Kefauver C, Payton JE, Vij R, et al.** Single-agent lenalidomide induces complete remission of acute myeloid leukemia in patients with isolated trisomy 13. *Blood.* 2009. **113**:1002–1005.

36. **Blum W, Klisovic RB, Becker H, Yang X, Rozewski DM, Phelps MA, Garzon R, et al.** Dose Escalation of Lenalidomide in Relapsed or Refractory Acute Leukemias. *JCO.* 2010. **28**:4919–4925.

37. **Wolschke C, Stübig T, Hegenbart U, Schönland S, Heinzelmann M, Hildebrandt Y, Ayuk F, et al.** Postallograft lenalidomide induces strong NK cell-mediated antimyeloma activity and risk for T cell-mediated GvHD: results from a phase I/II dose-finding study. *Exp. Hematol.* 2012. **41**:134–142.
38. **Kotla V, Goel S, Nischal S, Heuck C, Vivek K, Das B, Verma A.** Mechanism of action of lenalidomide in hematological malignancies. *J Hematol Oncol.* 2009; **2**:36.
39. **Benson DM Jr, Bakan CE, Zhang S, Collins SM, Liang J, Srivastava S, Hofmeister CC, et al.** IPH2101, a novel anti-inhibitory KIR antibody, and lenalidomide combine to enhance the natural killer cell versus multiple myeloma effect. *Blood.* 2011. **118**:6387–6391.
40. **Nowbakht P, Ionescu M-CS, Rohner A, Kalberer CP, Rossy E, Mori L, Cosman D, et al.** Ligands for natural killer cell-activating receptors are expressed upon the maturation of normal myelomonocytic cells but at low levels in acute myeloid leukemias. *Blood.* 2005. **105**:3615–3622.
41. **Abrams SI, Brahmi Z.** Target cell directed NK inactivation. Concomitant loss of NK and antibody-dependent cellular cytotoxicity activities. *J Immunol.* 1988. **140**:2090–2095.
42. **Jewett A, Bonavida B.** Target-induced anergy of natural killer cytotoxic function is restricted to the NK-target conjugate subset. *Cell. Immunol.* 1995; **160**:91–97.
43. **Gill S, Vasey AE, De Souza A, Baker J, Smith AT, Kohrt HE, Florek M, et al.** Rapid development of exhaustion and down-regulation of eomesodermin limit the antitumor activity of adoptively transferred murine natural killer cells. *Blood.* 2012. **119**:5758–5768.
44. **Gross CC, Brzostowski JA, Liu D, Long EO.** Tethering of intercellular adhesion molecule on target cells is required for LFA-1-dependent NK cell adhesion and granule polarization. *J. Immunol.* 2010. **185**:2918–2926.
45. **Rudnicka D, Oszmiana A, Finch DK, Strickland I, Schofield DJ, Lowe DC, Sleeman MA, et al.** Rituximab causes a polarisation of B cells which augments its therapeutic function in NK cell-mediated antibody-dependent cellular cytotoxicity. *Blood.* 2013. **121**:4694–4702.
46. **Floc'h AL, Jalil A, Vergnon I, Chansac BLM, Lazar V, Bismuth G, Chouaib S, et al.**  $\alpha E\beta 7$  integrin interaction with E-cadherin promotes antitumor CTL activity by triggering lytic granule polarization and exocytosis. *J Exp Med.* 2007. **204**:559–570.
47. **Franciszewicz K, Floc'h AL, Boutet M, Vergnon I, Schmitt A, Mami-Chouaib F.** CD103 or LFA-1 Engagement at the Immune Synapse between Cytotoxic T Cells and Tumor Cells Promotes Maturation and Regulates T-cell Effector Functions. *Cancer Res.* 2013. **73**:617–628.
48. **Li C, Ge B, Nicotra M, Stern JNH, Kopcow HD, Chen X, Strominger JL.** JNK MAP kinase activation is required for MTOC and granule polarization in NKG2D-mediated NK cell cytotoxicity. *PNAS.* 2008. **105**:3017–3022.
49. **Krzewski K, Chen X, Strominger JL.** WIP is essential for lytic granule polarization and NK cell cytotoxicity. *PNAS.* 2008. **105**:2568–2573.

50. **Liu D, Bryceson YT, Meckel T, Vasiliver-Shamis G, Dustin ML, Long EO.** Integrin-dependent organization and bidirectional vesicular traffic at cytotoxic immune synapses. *Immunity*. 2009. **31**:99–109.
51. **Hanaoka N, Jabri B, Dai Z, Ciszewski C, Stevens AM, Yee C, Nakakuma H, et al.** NKG2D initiates caspase-mediated CD3 $\zeta$  degradation and lymphocyte receptor impairments associated with human cancer and autoimmune disease. *J Immunol*. 2010. **185**:5732–5742.
52. **Breitkreutz I, Raab MS, Vallet S, Hideshima T, Raje N, Mitsiades C, Chauhan D, et al.** Lenalidomide inhibits osteoclastogenesis, survival factors and bone-remodeling markers in multiple myeloma. *Leukemia*. 2008. **22**:1925–1932.
53. **Schmiedel BJ, Nuebling T, Steinbacher J, Malinowska A, Wende CM, Azuma M, Schneider P, et al.** Receptor Activator for NF- $\kappa$ B Ligand in Acute Myeloid Leukemia: Expression, Function, and Modulation of NK Cell Immunosurveillance. *J Immunol*. 2012. **190**: 821–831.
54. **Schleypen JS, Von Geldern M, Weiss EH, Kotzias N, Rohrmann K, Schendel DJ, Falk CS, et al.** Renal cell carcinoma-infiltrating natural killer cells express differential repertoires of activating and inhibitory receptors and are inhibited by specific HLA class I allotypes. *Int. J. Cancer*. 2003. **106**:905–912.
55. **Alter G, Malenfant JM, Altfeld M.** CD107a as a functional marker for the identification of natural killer cell activity. *J. Immunol. Methods*. 2004. **294**:15–22.
56. **Schindelin J, Arganda-Carreras I, Frise E, Kaynig V, Longair M, Pietzsch T, Preibisch S, et al.** Fiji: an open-source platform for biological-image analysis. *Nature Methods*. 2012. **9**:676–682.

**FIGURE 1.** Characterizing primary AML blasts (dots), THP1 (blue line) and HL60 (red line) cell lines. **(A)** NK-cell ligand expression levels, expressed as the ratio of the mean fluorescence intensity (MFI) for each marker divided by the MFI for the negative controls, was determined on the indicated cell types by flow cytometry. For primary AML blasts, gating was done on CD33<sup>+</sup> cells in bone marrow or peripheral blood samples, each dot represents an individual sample out of 24. For THP1 and HL60 cells, lines represent the mean of three independent experiments. **(B)** Percentage of healthy donor NK cells degranulating in response to AML cells was determined by flow cytometry. After over-night co-incubation of PBMCs with AML cells in the presence of CD107a antibodies, percentage of CD107a<sup>+</sup> (i.e. degranulated) NK cells was assessed on the (CD3<sup>-</sup>CD56<sup>+</sup>) population in the lymphocyte's gate defined morphologically. Each symbol represents an individual experiment out of 24 for primary AML blasts and 5 for THP1 and HL60 cells. Bars represent means, \* $p < 0.05$ ; \*\* $p < 0.01$  (Mann-Whitney test). **(C)** Expression levels of NKG2D and DNAM-1 ligands, CD54 and CD11a were determined on THP1 and HL60 cell lines by flow cytometry. Representative histograms from one out of three independent experiments are shown.

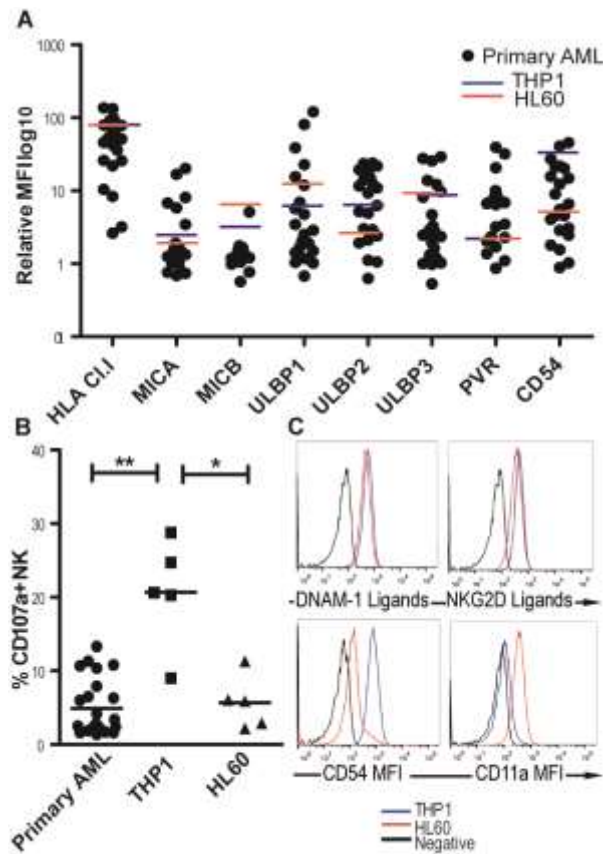


**FIGURE 2.** Effects of AML cells on NK-cell phenotype and function. PBMCs were co-cultured in round-bottomed 96-well plates alone or with irradiated AML cells (ratio 1:1). After 48 hours, PBMCs were phenotyped and tested for NK cell degranulation. **(A)** Receptor down-regulation on NK cells was assessed by flow cytometry, gating was done as indicated in Figure 1. Level of expression on NK cells cultured alone was compared with that on NK cells co-cultured with THP1 or HL60 myeloid cell lines, or with the control lymphoma cell line RAJI. Each symbol represents an individual experiment out of six, and mean  $\pm$  SD are shown. **(B)** PBMCs retrieved from cultures as described above were tested for degranulation against K562 as described in figure 1. Representative dot plot of one out of six are shown; for cells retrieved from culture alone (*upper left*), with THP1 cells (*upper right*) or with HL60 cells (*lower left*). In the graph (*lower right*) percentage of CD107a<sup>+</sup> NK cells after co-culture with THP1 or HL60 cells is presented. Each symbol represents an individual experiment. Bars represent mean  $\pm$  SD. \* $p < 0.05$ ; \*\* $p < 0.01$  (Wilcoxon's signed rank test). **(C)** Degranulation levels for IL-2-activated NK cells against primary AML blasts was measured as described in Figure 1 and correlated (Pearson correlation coefficient) with NKG2D down-regulation (MFI before/MFI after degranulation) on NK cells. MFI was assessed by flow cytometry as described in (A). **(D)** Conjugation tests were performed with purified NK cells stained with CellTracker Green (CMFDA) and THP1 or HL60 cells stained with CellTracker Orange (CMRA). Cells were mixed 1:1 and incubated for 1 h at 37°C. Percentage of bicolor cell-conjugates among CMFDA positive cells was measured by flow cytometry. Each symbol represents an individual experiment and bars represent mean  $\pm$  SD. \*\* $p < 0.01$  (Wilcoxon's signed rank test). **(E and F)** Experiments were performed as in (A and D), with PBMCs from three donors co-cultured with AML blasts isolated from four patients (Pt1 – Pt4). **(E)** DNAM-1, NKG2D and NKp46 levels were assessed after 48 hours of co-culture (*left*). Percentage of conjugates was also assessed (*right*). Plotted are means + SEM of the three PBMCs. \* $p < 0.05$ ; \*\* $p < 0.01$  (Mann-Whitney test). **(F)** Correlation between receptor down-regulation and the percentage of conjugates (Pearson correlation coefficient).

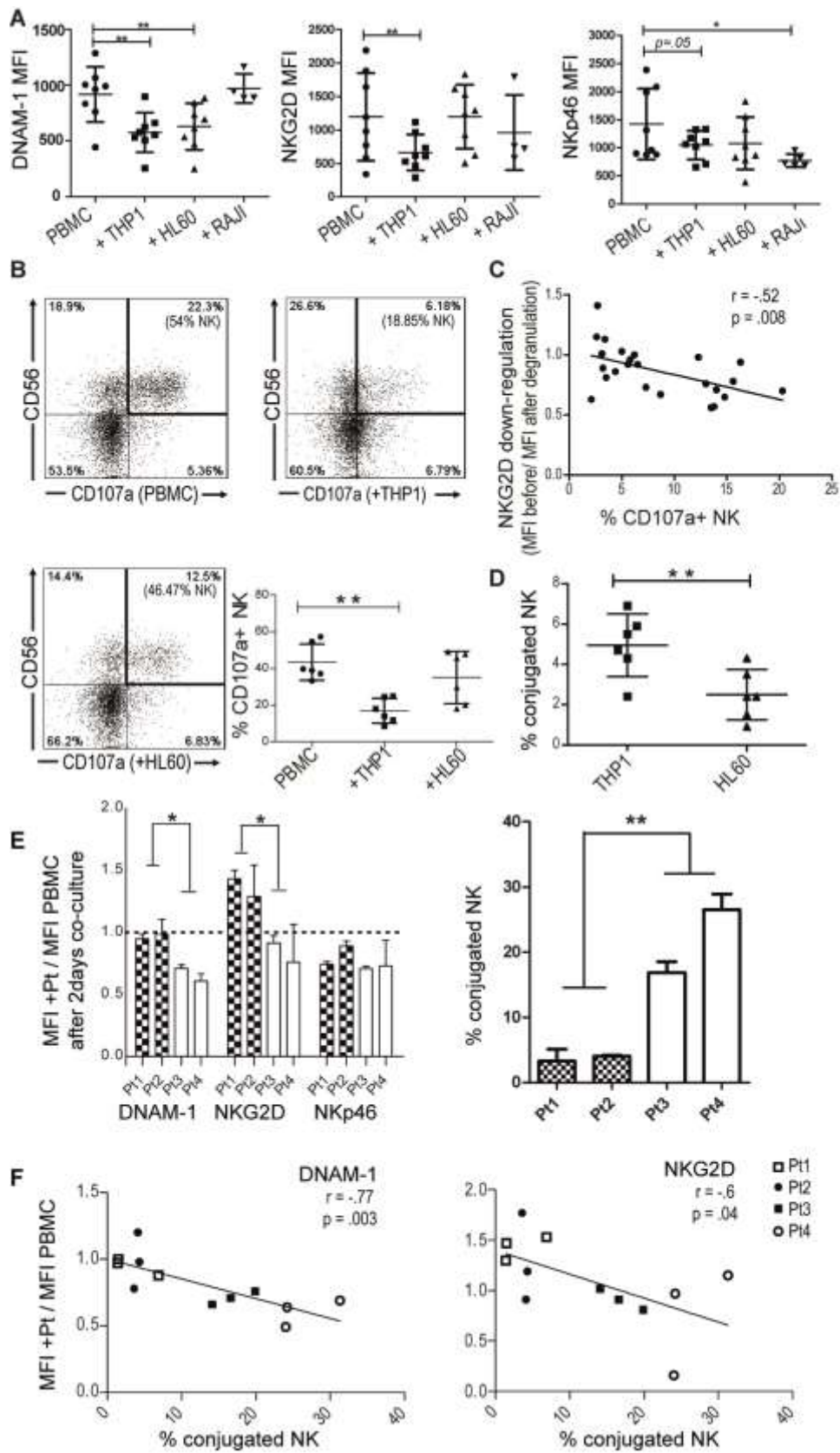


**Figure 2**

**FIGURE 3.** Time-lapse imaging of HL60 and K562 interactions with NK cells. In 3 independent experiments imaging was performed on a BioStation IM-Q (Nikon) at 40× magnification. Target cells (TCs) were manually tracked and interactions with NK cells (red) were scored for 137 K562 cells and 133 HL60 cells pooled from the 3 experiments. The time between conjugate formation and TC's killing, visualized by the appearance of intracellular fluorescence in TCs, was calculated. Timing (hh:mm:ss) started when NK cells were added to the plate. **(A)** Percentage of K562 or HL60 cells forming conjugates with NK cells was manually counted in images. \*\*\* $p < 0.0001$  (Fisher's exact test). **(B)** For comparison, percentage of NK-cell conjugates was also estimated by flow cytometry as described in Figure 2D. Each symbol represents an individual experiment and bars represent mean  $\pm$  SD. \*\* $p < 0.01$  (Mann-Whitney test). **(C)** Representative example of NK-cell interaction with HL60 cells, taken from the time-lapse experiences performed as described above: overlay (*upper row*), starting before the encounter (first frame to the left). In this example Conjugate-Kill time was 2 min 15 sec. *Lower row* presents blue channel fluorescence intensity in 16 colors. The trace represents the intensity profile in TC. **(D)** Conjugate-Kill time was determined for K562 and HL60 cells after contact with a single NK cell (mean 5 min 7 sec and 4 min 58 sec, respectively). NS: no significant difference (Mann-Whitney test). **(E)** Some TCs were hit by two NK cells; T1 is the Conjugate-Kill time for the first NK cell contact, and T2 the time for the second. Each symbol represents an individual TC. Data are shown as mean  $\pm$  SD and are pooled from the three time-lapse experiments. **(F)** Two examples of ineffective conjugates formed with HL60 cells; Overlaid time-lapse images taken as described above at 40× magnification: (*left*) initial contact, (*right*) NK cell leaving the HL60 cell undamaged (no blue fluorescence). Images are representative of 25 unkilld HL60 cells. **(G)** Percentage of K562 or HL60 cells surviving after forming at least one conjugate was manually counted in images. Data are pooled from the three time-lapse experiments. \*  $p = 0.04$  (Fisher's exact test).

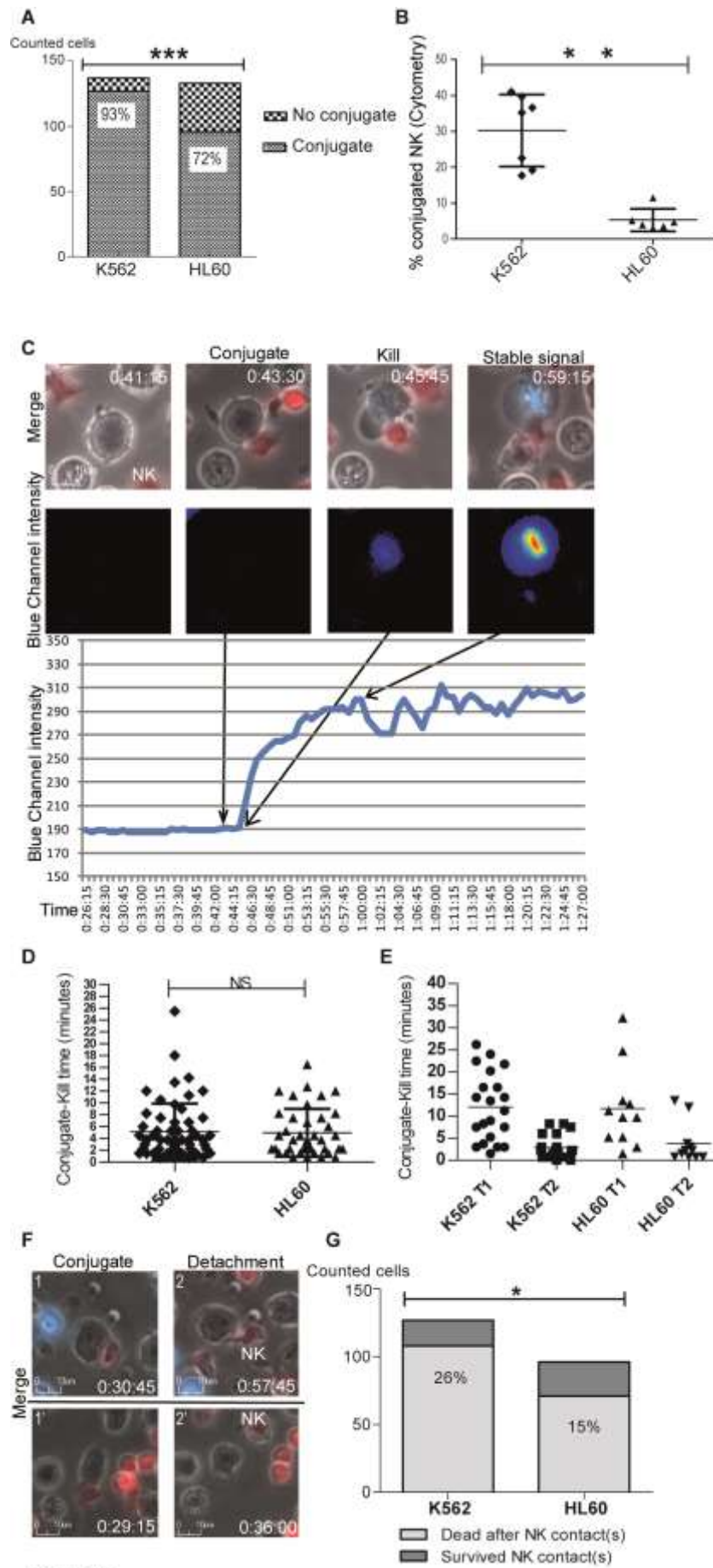
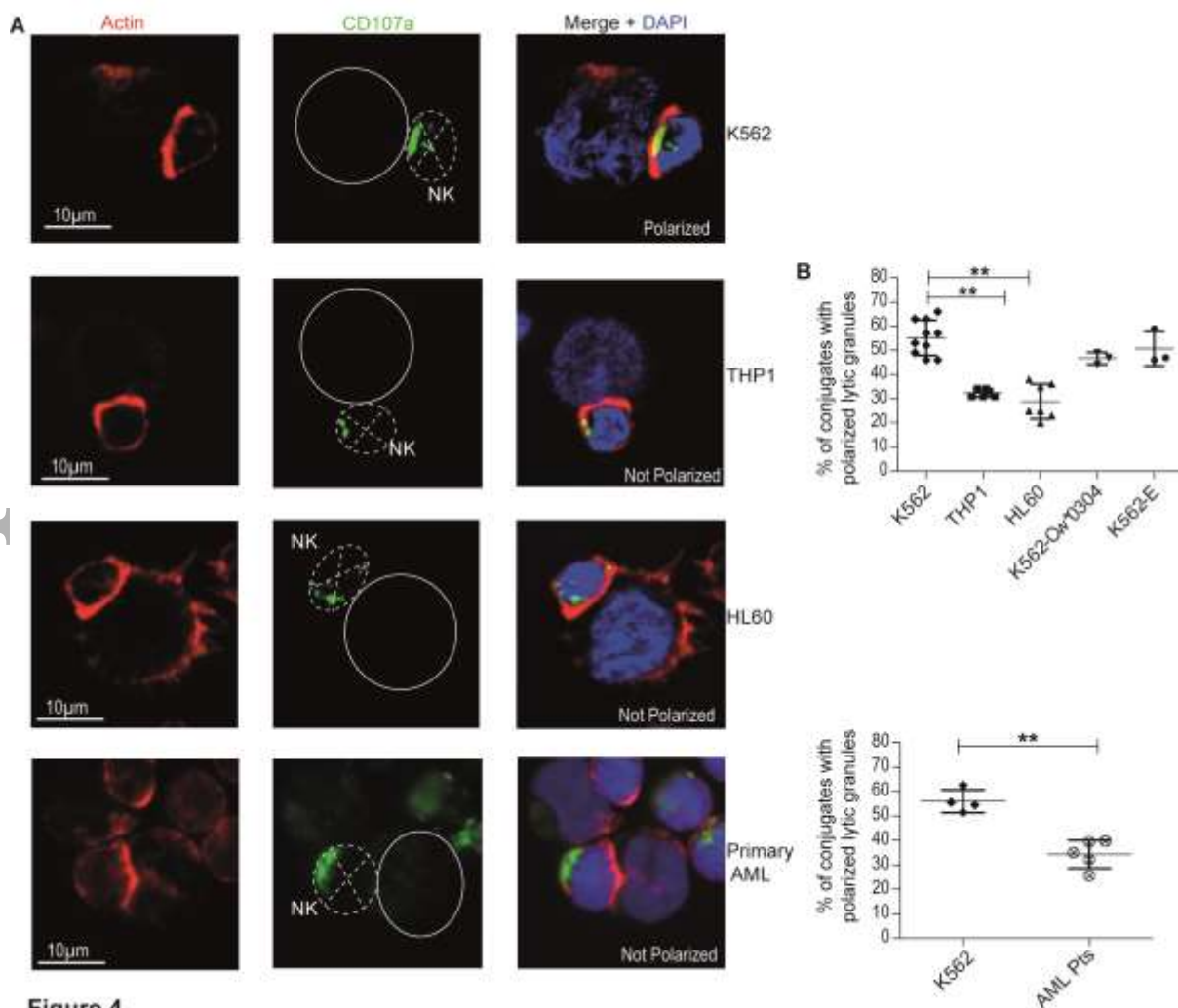


Figure 3

# Accepted Article

**FIGURE 4.** Lytic granule polarization in the NK-AML immunological synapse. Purified NK cells and AML cells were incubated together for 1 h at 37 °C, resuspended gently, seeded on slides, fixed and stained. Lytic granule (stained in green with antibody against CD107a) polarization was scored by counting under Axiovert 200M microscope (Carl Zeiss) in at least 50 NK/target cell conjugates in which F-actin had polymerized (*left panel*). Conjugates were considered polarized when CD107a<sup>+</sup> lytic granules were located in the quarter of the NK cell nearest the target cell (schematized in the *middle panel*). The *right panel* shows merge images with DAPI stain for nuclei. (A) Examples of conjugates with K562, THP1 and HL60 cells. Images were acquired with an LSM 510 confocal microscope at 64×/4 magnification, and are representative of 6 independent experiments. (B) Percentage of conjugates showing polarized lytic granules with AML cell lines (*upper graph*) or with AML patient (Pt) blasts (*lower graph*) compared with K562, K562-Cw\*0304 and K562-E the control cell lines, each symbol represents an experiment and means  $\pm$  SD are indicated. \*\* $p < 0.01$  (Wilcoxon's signed rank test).



**FIGURE 5.** Recruitment of LFA-1 and CD3 $\zeta$  in the NK-AML immunological synapse. LFA-1 (CD11a) or CD3 $\zeta$  recruitment to the contact area was estimated on slides prepared as indicated in Figure 4. Images were acquired with an Axiovert 200M microscope at 64 $\times$ /1.6 magnification. The relative recruitment index (RRI) in NK cells conjugated with K562, THP1 or HL60 cells was calculated as described in Materials and methods, where polymerized F-actin was visible (red, left). (A-B) Examples of NKIS with THP1 or HL60 cells. Recruitment of CD11a (green, middle) is shown in (A), and recruitment of CD3 $\zeta$  (green, middle) is shown in (B). The right panel shows merge images with DAPI stain for nuclei. Images are representative of three independent experiments. (C-D) RRI values for CD11a or CD3 $\zeta$ . Data are shown as mean  $\pm$  SD and are pooled from three different experiments, each point represents a cell. \*\*\* $p$  < 0.001 (unpaired t test). In the THP1 image in (B), an example of an NK cell (+) with no actin polarization is visible. This type of cell was not included in the counted conjugates.

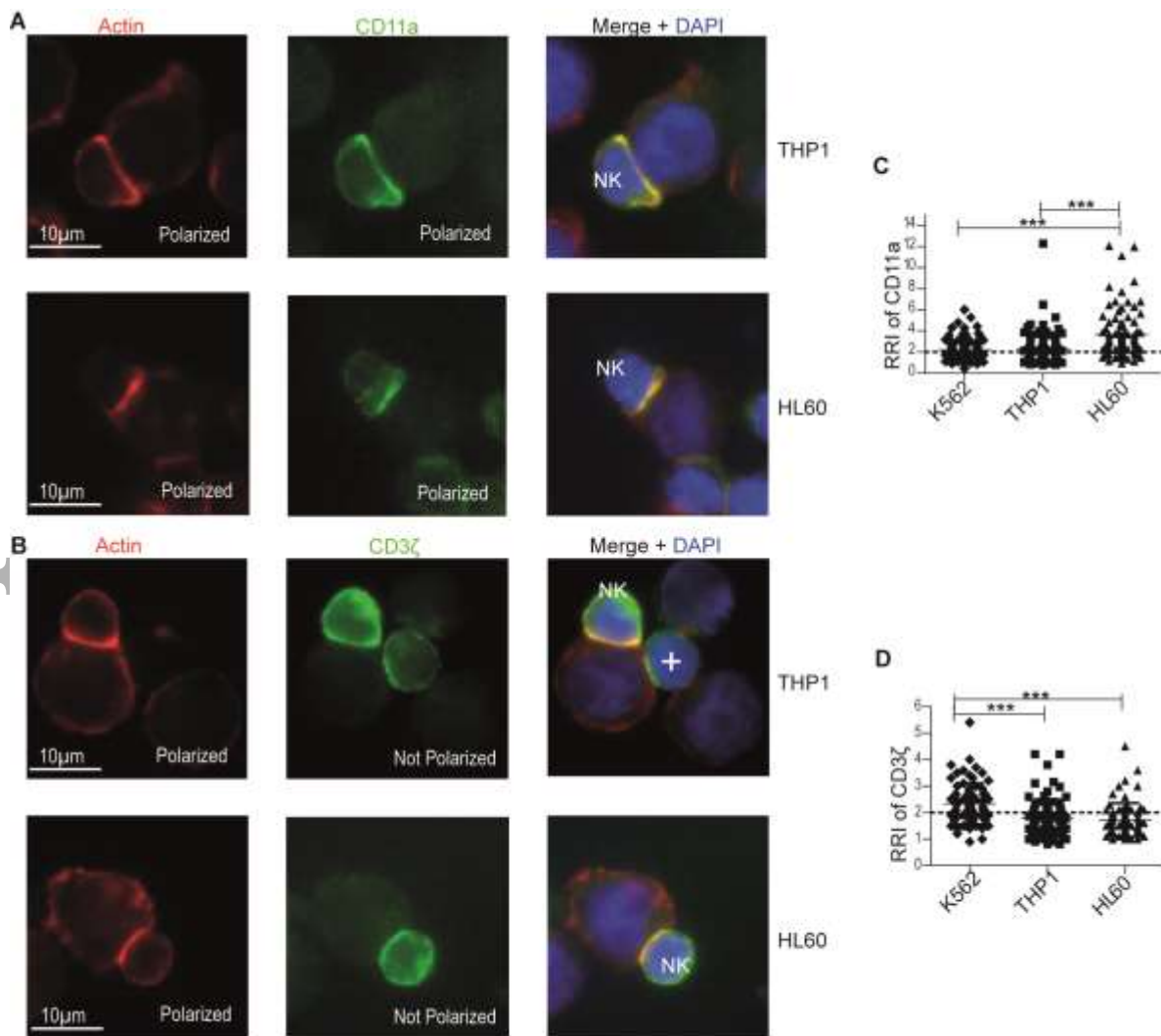


**Figure 5**

**FIGURE 6.** Relation of lytic granule polarization and CD3 $\zeta$  recruitment in the NK-AML synapse. **(A)** Purified NK cells and AML cells were incubated together for 1 h at 37 °C, resuspended gently, seeded on slides, fixed and stained for F-actin (red), CD3 $\zeta$  (green), and CD107a (blue). The right panel shows merge images. Images are representative of four independent experiments and were acquired with an LSM 510 confocal microscope at 64 $\times$ /4 magnification. **(B)** Lytic granule polarization was evaluated in NK-AML conjugates with (RRI > 2) or without (RRI < 2) CD3 $\zeta$  recruitment, as described in Figure 4. The number of NK cells with or without CD107a polarization is shown in conjugates with THP1 cells (upper graph) or with HL60 cells (lower graph). Data are pooled from three experiments. \*\*\*  $p$  < 0.001 (Fisher's exact test).

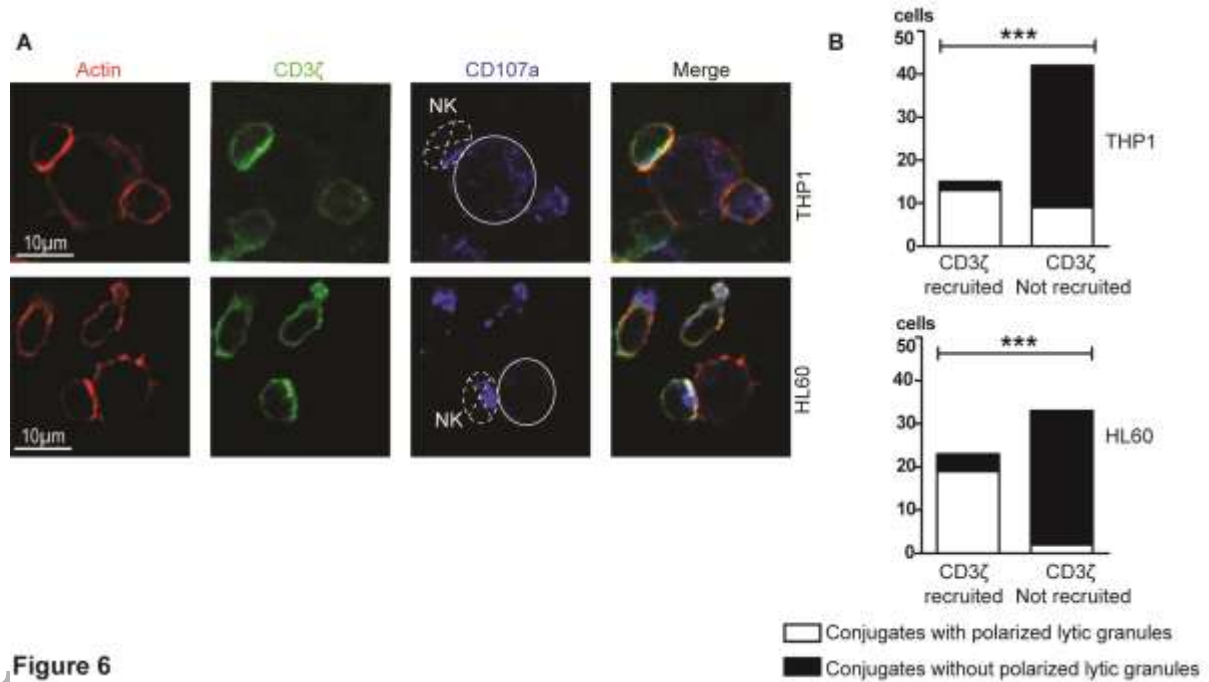
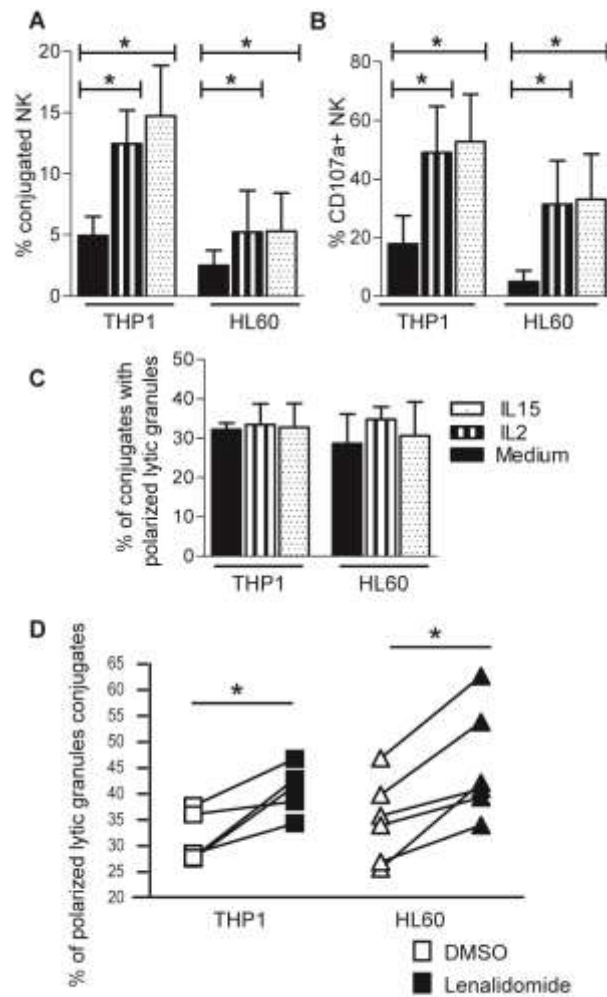


Figure 6

**FIGURE 7.** Effects of AML cell lines treatment with lenalidomide or NK-cell pre-activation with IL-2 or IL-15 on NK-cell degranulation. **(A-C)** NK cells were activated overnight with 10 ng/mL IL-15 or 1000 UI/mL IL-2 before **(A)** using flow cytometry to assess the number of conjugates formed as indicated in Figure 2, **(B)** determining the NK degranulation rate by flow cytometry as described in Figure 1, and **(C)** determining the percentage of conjugates showing granule polarization by microscopy as indicated in Figure 4. Data are shown as mean + SD of six independent experiments. **(D)** Lenalidomide was added to THP1 and HL60 cell lines cultures at 10  $\mu$ M 18-24 hours before using microscopy to assess lytic granule polarization as described in Figure 4. Results are compared with control where only the solvent DMSO was added. Each symbol represents an individual experiment from six performed. \* $p < 0.05$  (Wilcoxon's signed rank test).



**Figure 7**